This article has been accepted for publication in a future issue of this journal, but has not been fully edited. Content may change prior to final publication. Citation information: DOI 10.1109/LAWP.2020.3009453, IEEE Antennas and Wireless Propagation Letters

Chipless RFID Tag with Enhanced RCS Used as a Phthalocyanine-Based Solvent Vapors Sensor

Milan Svanda, Jan Machac, *Senior Member, IEEE*, Milan Polivka, *Member, IEEE*, Sarka Havlova, Premysl Fitl, Martin Vrnata

***Abstract*—A novel uniplanar chipless RFID solvent vapors/gas sensor is proposed in this paper. The sensor etched on an extremely thin capton substrate is composed of the folded dipole resonator loaded by the interdigital capacitor located inside the planar rectangular metallic loop that improves the RCS response. When illuminated by a plane wave, the folded dipole causes a notch in the RCS response of the loop located near its resonant frequency. The high RCS level (-18 dBsm), together with the notch depth (16 dB) assure a reliable detection of its position within the frequency dependence of RCS curve. In order to enhance the structure sensitivity to the presence of acetone vapors, the tetrasulfonated copper phthalocyanine thin film was applied as a sensitive layer during the process of folded dipole metallization. The experimental verification confirmed the viability of sensor proof-of-concept for the detection of chemical vapors.**

***Index Terms*—Chipless RFID, radar cross section, resonant elements, sensors.**

I. Introduction

THE RFID technology is currently spread into an increasing number of human activities. Apart from the reliability of lossless objects identification [1], other complex challenges need to be addressed, such as tracking and sensing applications, operation of tags attached to lossy dielectric and metallic objects [2], identification of human tissue [3-5], as well as integration of RFID tags with sensors [6-7]. The chipless RFID represents a special class of such technology, combining the benefits of remote sensing of common chip RFID arising from the employment of simple printed and low-cost tags; [8-19].

The new and perspective approach with a strong application potential is represented by chipless RFID transponders with sensing capability; [20-30]. Issues to be solved for reliable employment of sensor chipless tags are similar to those in the case of identification chipless RFID tags. The advantage of sensor tags consists in a relatively small bit capacity requested. On the contrary, the tag sensitivity to measured quantity constitutes the fundamental performance parameter.

The main problem connected with the design of chipless RFID sensor as well as identification tags is to assure a sufficiently high radar cross section (RCS) to enable the tag response detection at the requested distance [12]. The second important problem is to assure the proper operation of the tag in real environment – often especially in the presence of metallic objects that can mask the required reflections from the tag by their own strong false reflections [18]. The tags that enable to reduce these false reflections can be based e.g. on resonators array situated at a specific distance above the ground plane [16-18]. The other possibility is to design resonators in the form of slots in the metal plate [19]. In both cases, the coded information is shown as notches in the reflection response (RCS) caused by the metal ground patch.

The theoretical principles of remote gas sensing within GHz frequency are reported in [31]. The resonator substrate is equipped with interdigital electrodes and a disconnected path between them. While the sensitive layer covering interdigital electrodes generates a certain capacity, another part of the sensitive layer covering the disconnected path generates a certain inductance. There is an influence of various molecular parameters on the alteration of either capacity or inductance of LC-resonator. To give several examples: (molecular dipole moment → capacity [32-36], ability to exchange electrons → inductance; ability to form hydrogen bond → inductance) [31].

This paper presents a new version of planar resonators that behave in a similar way as dipoles located above the metallic patch presented in [18]. Here, the patch is replaced by a metallic loop equipped with the resonator, represented by a shortened U-folded dipole (UD) loaded with a meander capacitor placed inside its geometry to keep the external shape intact. The whole structure is etched on an extremely thin (25 μm) capton substrate, thus remains uniplanar. Such configuration improves the RCS of structure up to the level of about -18 dBsm (compared to the case of standalone UD). The U-dipole resonator creates in the frequency response of the loop a notch of the depth of about 16 dB. To our best knowledge, this is the first time the thin film of phtalocyanine derivatives (in this case, the tetrasulfonated copper phthalocyanine) has been applied as a sensitive layer in order to improve the structure sensitivity to acetone vapors. The resulting sensor tag can be potentially applied in chemical industry for low-cost wireless identification of undesirable solvent vapors.

Manuscript received in June, 2020; accepted July, 2020. Date of publication xx. This work has been supported by the Czech Science Foundation partially under projects No. 17-02760S (analysis and simulation) and No. 20-02046S (experiments).

M. Svanda, J. Machac, and M. Polivka are with the Department of Electromagnetic Field, Faculty of Electrical Engineering, Czech Technical University in Prague, Technicka 2, 166 27 Prague, Czech Republic (e-mail of the corresponding author: svanda.milan@fel.cvut.cz).

S. Havlova, P. Fitl, and M. Vrnata are with the University of Chemistry and Technology Prague, Faculty of Chemical Engineering, Department of Physics and Measurements, Technicka 5, 166 28 Prague, Czech Republic.

Digital Object Identifier inserted by IEEE

This article has been accepted for publication in a future issue of this journal, but has not been fully edited. Content may change prior to final publication. Citation information: DOI 10.1109/LAWP.2020.3009453, IEEE Antennas and Wireless Propagation Letters

II. PROPERTIES OF U-SHAPED DIPOLE TYPE RESONATORS

Fundamental performance parameters for chipless RFID sensor tags are defined in Fig. 1. The frequency shift Δf was simulated by means of 0.1 mm thin layer with the relative permittivity $\varepsilon_r = 3$ spread on the analyzed structure. The comparison of key parameters of various simple folded dipole type resonators is presented in Fig. 2. All structures were simulated on the standard 0.76 mm thick Rogers RO4350B substrate with the relative permittivity equal to 3.66. To make an accurate comparison, all of them were tuned to the same frequency of 3 GHz. The shortened U-folded dipole terminated by an interdigital capacitor (IC UD) can be selected as a good candidate for follow-up development steps. The IC UD embodies a very small electrical size *ka*; see Fig. 2a, high sensitivity Δf; Fig. 2d, sufficient peak height $h = 20$ dB and an adequately high-quality factor reaching about $Q \sim 200$; Fig. 2c, that is inversely proportional to the BW; [37]. A very low RCS level (< -70 dBsm) constitutes the trade-off expense. However, this parameter can be substantially improved by coupling the IC UD to a larger metallic structure (e.g. metallic rectangular loop) as described in the next section.

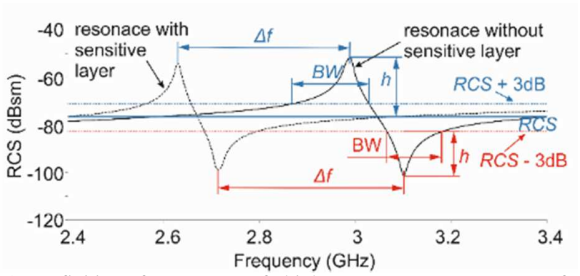

Fig. 1. Definition of parameters of chipless RFID sensor scatterers of peak (blue) and drop (red) resonance type.

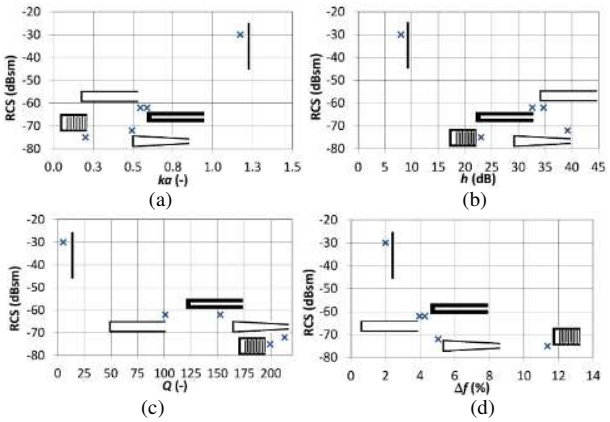

Fig. 2. Comparison of basic U-shaped dipole type scatterers according to RCS and (a) resonance *ka* product, (b) peak hight *h*, (c) quality coefficient *Q*, (d) sensitive layer frequency offset Δf.

III. ENHANCEMENT OF INTERDIGITAL SHORTENED U-SHAPED DIPOLE RESONATOR RCS RESPONSE

A. Standalone loop properties

A metallic rectangular loop was selected in order to raise the overall tag RCS level. Unlike the size of metallic area, it is not essential to change the loop geometry in order to improve the RCS. The rectangular loop geometry was selected, because it is easy to locate the U-dipole into its inner part. The properties of standalone loop without IC UD resonator were analyzed from the frequency dependence of its RCS curve. It was observed that the loop width w_{strip} represented the crucial parameter for reaching the flat RCS characteristic; see Fig. 3. The narrower loop strip w_{strip}, the sharper RCS characteristic, whereas the wider loop strip, the flatter the RCS characteristic. The final loop geometry was selected as a trade-off between the flat RCS characteristic on one hand and the acceptable tag dimension together with the sufficient space inside the loop for IC UD placement on the other hand.

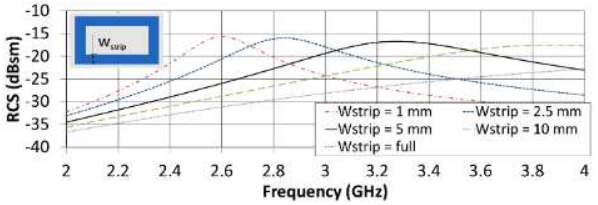

Fig. 3. Dependence between simulated loop RCS and loop strip width w_{strip}.

B. IC UD coupled to the loop

The IC UD resonator coupled into a metallic loop can be seen in Fig. 4. The number of interdigital fingers of the folded UD termination variates the loading capacitance, and consequently the resonant frequency. This effect can be used in a sensor at which the measured/detected quantity modulates the value of capacitor loading the folded dipole. The notch in the RCS response caused by the IC UD resonator can be clearly detected as its depth ranges from 8 to 20 dB.

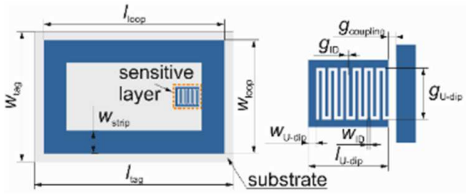

Fig. 4. Resonant element and IC U-dipole coupled inside the metallic loop.

The notch depth in the RCS response of structure depends on the resonator position inside the loop - as plotted in Fig. 5. The most sensitive RCS response has been obtained for the dipole placed in the immediate proximity of the shorter loop sides. That is due to the strong coupling between the IC UD and the loop at the moment when the structure is exposed to a plane wave. But, conversely, when the IC UD is placed in the loop center, the response is very small.

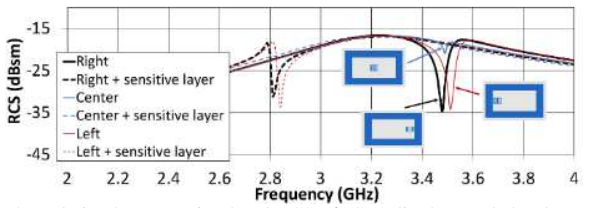

Fig. 5. Relation between simulated RCS of IC U-dipole coupled to loop and its position inside the loop.

Fig. 6 depicts the RCS of IC UD coupled to the loop in the dependence on the number of interdigital strips *N*. It can be observed that the increase in value of *N* has two positive effects. Firstly, it enhances the sensitivity Δf and, secondly, it slightly increases the quality factor *Q*. Other parameters have no significant influence on the monitored quantities.

This article has been accepted for publication in a future issue of this journal, but has not been fully edited. Content may change prior to final publication. Citation information: DOI 10.1109/LAWP.2020.3009453, IEEE Antennas and Wireless Propagation Letters

The improvement in the fundamental sensor parameter Δf was achieved thanks to the extremely thin 25 µm capton substrate with the relative permittivity equal to 3.0. Due to the low substrate thickness, the effective permittivity in the close vicinity of the sensitive layer is reduced. Consequently, the higher intensity of electromagnetic field affected the layer.

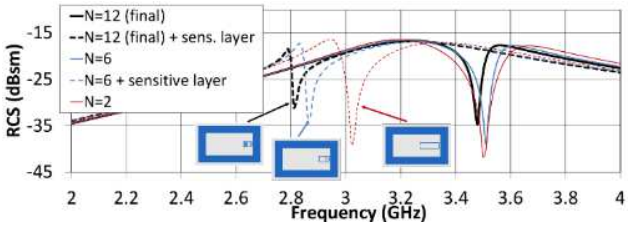

Fig. 6. Dependence between imulated RCS of IC U-dipole coupled to the loop and number of interdigital strips *N*.

C. *Design of the sensor tag based on IC UD coupled to the loop*

The resonator destined to serve as a gas sensor was fabricated on the Dupont Pyralux AP 8515R substrate with the relative permittivity equal to 3.0; see Fig. 7a. In order to raise the sensor sensitivity, we decided to employ a very thin substrate whose thickness counts only 25 µm. The parameters of folded UD located at the distance of 2 mm from the inner loop edge ($g_{coupling}$) are as follows: width of loop strips $w_{strip} = 5$ mm and outer dimensions $l_{loop} \times w_{loop}$ are 40 × 25 mm, length of folded dipole arms $l_{UD} = 5.3$ mm, their width $w_{UD} = 0.5$ mm, distance between them $g_{UD} = 3.4$ mm. There are $N = 12$ fingers of terminating capacitor of 0.2 mm in width w_{ID}, in the distance of $g_{ID} = 0.2$ mm from each other. The sensitive phthalocyanine layer with properties indicated in Table I was placed on the IC UD motif area.

The E-field is coupled between the U-folded dipole and the loop in the similar way as it is coupled between interdigital fingers. The maximum intensity is obviously located by the inner edge of rectangular loop, which gives rise to a strong coupling creating a resonant drop in the loop RCS response; see Fig. 7b.

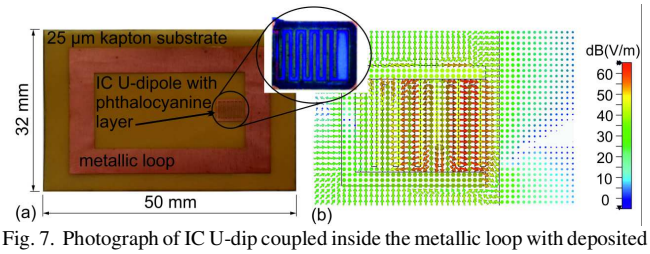

Fig. 7. Photograph of IC U-dip coupled inside the metallic loop with deposited CuPcTS sensitive layer (a) and detail with E-field intensity (b).

Fig. 8 depicts the RCS response of final design of IC UD coupled to the loop, simulated with the help of the MoM method (full-wave simulator Zeland IE3D). To illustrate the sensitivity improvement, we compare it with the version designed on the standard 0.76 mm thick Rogers RO4350B substrate with the relative permittivity ε_r equal to 3.66. Two simulations, i.e. without the sensitive layer and with the sensitive layer, situated on the sensor tag motif were performed for both designs. The sensitive layer was simulated as infinitely extended 0.1 mm thick layer with $\varepsilon_r = 3.0$ (as a consequence of solver implementation). This model differs partly from the measured phthalocyanine layer, yet for the relative comparison of particular cases, it provides the sufficient information. As it was verified, the layer outside the UD resonator area has only a minor influence on the frequency shift Δf.

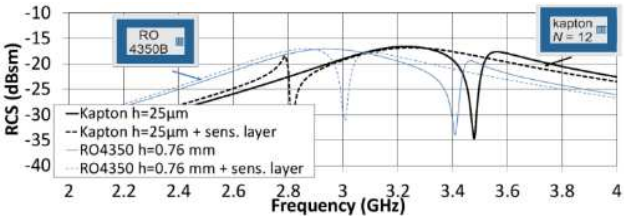

Fig. 8. Comparison between the simulated RCS response of IC U-dipole coupled to the loop on the 25 µm capton substrate and Rogers substrate of 0.76 mm in thickness.

IV. Sensitive Chemical Phthalocyanine Layers

The sensitive layer represents an essential part of tag's sensing function. Based on the analysis of properties of potentially applicable substances and our previous experience with phthalocyanines [38, 39], we used the latter in production of active sensing films of proposed tags. Phthalocyanines are organic macrocyclic molecules with a summary formula $(C_8H_4N_2)_4$. They consist of four isoindole heterocycles connected by nitrogen bridges into one macrocycle with four nitrogen atoms in the center. The center cavity can be occupied by more than 70 various metallic cation types, forming phthalocyanine derivatives called metallophthalocyanines. Basic metallophthalocyanies are intensively colored compounds with the known applicability as selective sensing films or films for organic photovoltaics. Their sensing response is based on the change of impedance in the presence of detected gaseous analyte. However, the basic metallophthalocyanines suffer from a very low solubility in polar and nonpolar solvents. The modification of isoindol cycles by various substituents (e.g. sulfo $–SO_3H$ group) constitutes a promising way how to improve their solubility and sensing response. The metallophtalocyanines modified in the foresaid manner are soluble in water. Based on the above-mentioned facts, we chose the tetrasulfonated copper phthalocyanine (copper (II) phthalocyanine-3,4´,4´´,4´´´- tetrasulfonic acid tetrasodium salt – abbreviated as CuPcTS) as the active film. The solution of the respective phthalocyanine in distilled water was prepared in the concentration of 1.45 mmol/l. Two variants of sensitive layer were applied by pipetting and subsequent drying with the volume of 15 µl and 30 µl, respectively; see Tab I. The resulting CuPcTS film deposited on the sensor substrate is depicted in Fig. 7.

V. Sensor Tag Measurement

The verification of sensor tags sensitivity was performed by measurement in the R32 waveguide line by the VNA Agilent E8364A. The tag was inserted horizontally into the waveguide chamber. This "tested gas section" was separated from the other measurement line parts by tedlar membranes in order to hermetically insulate the solvents vapor; see Fig. 9. The defined 10 000 ppm concentration of acetone vapor in the synthetic air was introduced to the "tested gas section" by a suction pump that supplied it from the tedlar bag.

This article has been accepted for publication in a future issue of this journal, but has not been fully edited. Content may change prior to final publication. Citation information: DOI 10.1109/LAWP.2020.3009453, IEEE Antennas and Wireless Propagation Letters

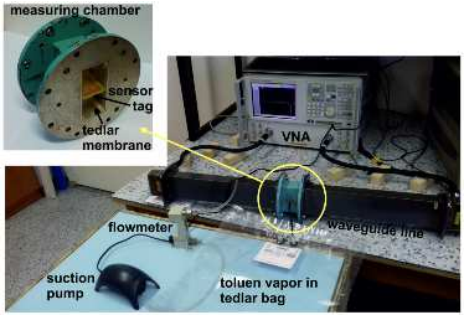

Fig. 9. Photograph of measurement setup, detailing the measuring chamber and sensor tag position.

In Table I you can see the comparison of measurements regarding IC UD coupled to the loop and separate IC UD for two sensitive layer thicknesses. Fig. 10 depicts the scattering response of IC U-dipole coupled to the loop with the CuPcTS sensitive layers with- and without- the 10 000 ppm acetone vapor, measured through the reflection coefficient of waveguide line. There are significant frequency shifts accounting for 7.1 and 10.2 MHz (caused by the presence of acetone vapor) that are attributable to sensitive phthalocyanine layer of 0.6 and 1.2 μm in thickness, respectively. Consequently, the functionality of the above-proposed sensing mechanism as well as the RCS response enhancement of the structure were verified.

TABLE I
MEASURED FREQUENCY SHIFT DEPENDING ON STRUCTURE GEOMETRY AND PARAMETERS OF PHTHALOCYANINE SENSITIVE LAYERS

#	Tag type	Phthalocyanine layer thickness (μm)	Phthalocyanine layer volume (μl)	Δf (MHz)	Δf (%)
1	IC U-dip	0.6	15	5.8	0.20
2		1.2	30	7.2	0.25
3	Loop IC U-dip	0.6	15	7.1	0.21
4		1.2	30	10.2	0.30

Apart from the sensitivity measurement of the proposed tag in the waveguide line chamber, the direct verification of RCS response was performed by monostatic measurement in anechoic chamber; see Fig. 11. It was based on the reflection coefficient evaluation of the double ridge horn antenna DRH20 [40] in front of which a transponder at the distance of 0.5 m was placed. The tag's RCS response was calculated according to the relation used in [10] and modified so that it was applicable to the one-port measurement described in [13]. The enhanced RCS response level of about -18 dBsm as well as significant drop depth better than 15 dB were confirmed.

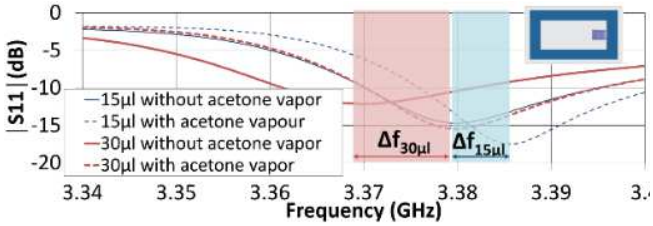

Fig. 10. Measured scattering response of IC U-dipole coupled to the loop with phthalocyanine sensitive layers with and without the 10 000ppm acetone vapor measured through reflection coefficient of waveguide line.

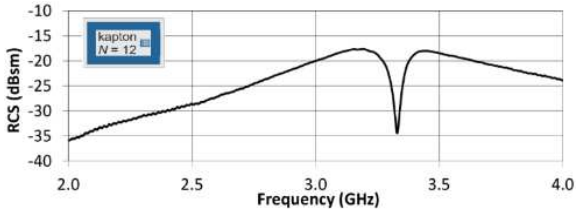

Fig. 11. RCS response of the IC U-dipole coupled to the loop without sensitive layer measured in an anechoic chamber.

Table II compares properties of this solution with published acetone sensors operating within the microwave frequency band. Although the relative sensitivity of the presented solution is lower than the results published by authors, these structures are mostly detected by direct cable measurement or, in few cases, wirelessly from a short distance. In fact, the remote sensing structure proposed in our paper shows the improved RCS response, which overcomes the referenced competitors. This can be considered the main contribution of the paper. The future research will address the issue of performance improvement in sensitive phthalocyanine layer.

TABLE II
COMPARISON OF PROPERTIES OF MICROWAVE ACETONE SENSORS

Type of sensor structure	f_0 (GHz)	Δf (kHz/ppm)	RCS (dBsm)	Notch (dB)	Contact-less
[32] Microstrip line	8.5	15 200	-	-	No
[34] Ring resonators	4	40	-30	14	15 mm
[35] Split-ring reson.	5.5	30	-25	10	No
[36] Open gap reson.	7.4	17	-	-	No
This work: UD in loop	3.4	1.2	-18	16	500 mm

VI. CONCLUSION

This paper presents the results of investigation of the novel uniplanar resonator, which can be used as a chipless RFID chemical gas sensor. The resonator is composed of the U-folded dipole terminated by the interdigital capacitor coupled inside the rectangular metallic loop that assures a sufficiently high RCS response of ca. -18 dBsm. The U-folded dipole resonator causes a notch of 16 dB in the RCS characteristics that is superimposed to the loop's RCS characteristics, which can be easily detected. The tetrasulfonated copper phthalocyanine thin film (applied as a sensitive layer above the folded dipole) enhances the structure sensitivity. The experimental verification confirmed the viability of the sensor's proof-of-concept for detection of chemical vapors.

The future work will be concentrated on the detailed research of sensitive chemical sensor layers as well as development of a measuring chamber for free space measurement of chemical vapors. The waveguide measurement was used to verify the sensing mechanism and to ensure the reproducible detection of the defined vapor concentration. Nevertheless, it can be stated that the properties of tag itself have been reliably verified and will be retained even when located in the free space. The future work will focus on the open space measurements and investigation of methods of further increase in sensor sensitivity. The tag's virtue consists in its possible use as a simple and cheap wireless uniplanar sensor applicable e.g. in chemical industry for the detection of occurrence of harmful gases or solvent vapors.

REFERENCES

[1] K. Finkenzeller, "*RFID Handbook: fundamentals and applications in contactless smart cards and identification*," 2nd edition, John Wiley & Sons, 2005.

[2] A. Ali Babar *et al.*, "Small and flexible metal mountable passive UHF RFID tag on high-dielectric polymer-ceramic composite substrate," *IEEE Antennas Wireless Propag. Lett*., no. 11, pp. 1319-1322, 2012.

[3] G. Marrocco, "RFID antennas for the UHF remote monitoring of human subjects," *IEEE Trans. Antennas Propag*., vol. 55, no. 6, pp. 1862-1870, Jun. 2007.

[4] M. Svanda and M. Polivka, "Two novel extremely low-profile slot-couplet two-element patch antennas for UHF RFID of people," *Microw. Optical Tech. Lett.*, vol. 52, issue 2, pp. 249-252, 2010.

[5] M. Svanda and M. Polivka, "Horizontal five-arm folded dipole over metal screening plane for UHF RFID of dielectric objects," *Microw. Optical Techn. Lett*., vol. 52, no. 10, pp. 2291-2294, Jul. 2010.

[6] C. Occhiuzzi, S. Caizzone, and G. Marrocco, "Passive UHF RFID antennas for sensing applications: Principles, methods and classifications," *IEEE Antennas Propag. Mag*., vol. 55, no. 6, pp. 14-34, Dec. 2014.

[7] J. Kracek *et al.*, "Implantable semi-active uhf rfid tag with inductive wireless power transfer," *IEEE Antennas Wireless Propag. Lett.*, vol. 15, issue 1, pp. 1657-1660, 2016.

[8] N. Ch. Karmakar, "Tag, you're it radar cross section of chipless RFID tags," *IEEE Microw. Mag.*, vol. 17, no. 7, pp. 64-74, Jun. 2016.

[9] M. Forouzandeh and N. Ch. Karmakar, "Chipless RFID tags and sensors: a review on time-domain techniques," *Wireless Power Transf.*, vol. 2, Special issue 2: Chipless Technologies, pp. 62-77, 2015.

[10] A. Vena, E. Perret, and S. Tedjini, "A fully printable chipless RFID tag with detuning correction technique," *IEEE Microw. Wireless Comp. Lett.*, vol. 22, no. 4, pp. 209-211, Mar. 2012.

[11] O. Rance *et al.*, "Toward RCS magnitude level coding for chipless RFID," *IEEE Trans. Microw. Theory Techn.*, vol. 64, no. 7, pp. 2315-2325, May 2016.

[12] M. Polivka, J. Havlicek, M. Svanda, and J. Machac, "Improvement of RCS response of U-shaped strip-based chipless RFID tags." In Conference Proc. - European Microwave Week 2015 (45th EuMC, EuRAD, EuMIC, EuWT) [CD-ROM], 2015.

[13] J. Havlicek *et al.*, "Chipless RFID tag based on electrically small spiral capacitively loaded dipole," *IEEE Antennas Wireless Propag. Lett.,* vol. 16, pp. 3051 - 3054, 2017.

[14] H. Huang and L. Su, "A compact dual-polarized chipless RFID tag by using nested concentric square loops," *IEEE Antennas Wireless Propag. Lett.,* vol. 16, pp. 1036 - 1039, Oct. 2017.

[15] M. Added *et al.*, "High-performance chipless radio-frequency identification tags: using a slow-wave approach for miniaturized structure," *IEEE Antenn. Propag. Mag*., vol. 61, issue 4, pp. 46 - 54, 2019.

[16] F. Costa, S. Genovesi, and A. Monorchio, "A chipless RFID based on multiresonant high-impedance surfaces," *IEEE Trans. Microw. Theory Techn.*, vol. 61, no. 1, pp. 146–152, Dec. 2013.

[17] J. Kracek, M. Svanda, and K. Hoffmann, "Scalar method for reading of chipless rfid tags based on limited ground plane backed dipole resonator array," *IEEE Trans. Microw. Theory Tech.*, vol. 67, issue 11, pp. 4547-4558, 2019.

[18] M. Svanda *et al.*, "Platform tolerant, high encoding capacity dipole array-plate chipless rfid tags," *IEEE Access*, vol. 7, issue 1, pp. 138707-138720, 2019.

[19] J. Havlicek *et al.*, "Improvement of reading performance of frequency domain chipless rfid transponders," *Radioengineering*, vol. 25, no. 2, pp. 219-229, 2016.

[20] N. Ch. Karmakar, E. M. Amin, and J. M. Saha, "*Chipless RFID sensors*," John Wiley & Sons, pp. 16-21, 2016.

[21] D. Girbau *et al.*, "Passive wireless temperature sensor based on time-coded UWB chipless RFID tags," *IEEE Trans. Microwave Theory Tech.*, vol. 60, issue 11, pp. 3623 – 3632, 2012.

[22] Y. Feng *et al.*, "Flexible UHF resistive humidity sensors based on carbon nanotubes," *IEEE Sensors Jour.*, vol. 12, issue 9, pp. 2844 – 2850, 2012.

[23] A. M. J. Marindra and G. Y. Tian, "Chipless RFID sensor tag for metal crack detection and characterization," *IEEE Transactions on Microwave Theory and Techniques*, vol. 66, issue 5, pp. 2452 – 2462, 2018.

[24] S. Shrestha *et al.*, "A chipless RFID sensor system for cyber centric monitoring applications," *IEEE Trans. Microw. Theory Tech.*, vol. 57, issue 5, pp. 1303 – 1309, 2009.

[25] C. Occhuizzi, "RFID passive gas sensor integrating carbon nanotubes," *IEEE Trans. Microw. Theory Tech.* vol 59, issue 10, pp. 2674-2684, 2011.

[26] A. A. Kutty, "A novel carbon nanotube loaded passive uhf rfid sensor tag with built-in reference for wireless gas sensing," IEEE MTT-S Int. Microw. Symp. (IMS), San Francisco, USA, 2016.

[27] A. Jiménez-Sáez *et al.*, "Chipless Wireless High Temperature Sensing Based on a Multilayer Dielectric Resonator," 2019 *IEEE Sensors*, Montreal, QC, Canada, 2019, pp. 1-4.

[28] Z. Li and S. Bhadra, "A Flexible Printed Chipless RFID Tag for Concentration Measurements of Liquid Solutions," 2019 *IEEE Sensors*, Montreal, QC, Canada, 2019, pp. 1-4.

[29] A. Vena, *et al.*, "Toward a Reliable Chipless RFID Humidity Sensor Tag Based on Silicon Nanowires," *IEEE Trans. Microwave Theory Tech.*, vol. 64, no. 9, pp. 2977-2985, 2016.

[30] A. Vena *et al.*, "A Fully Inkjet-Printed Wireless and Chipless Sensor for CO2 and Temperature Detection," *IEEE Sensors Jour.*, vol. 15, no. 1, pp. 89-99, 2015.

[31] B. Fonseca *et al.,* "Microwave signature for gas sensing: 2005 to present," *Urban Climate*, vol. 14, pp. 505-515, 2015.

[32] A. Rydosz *et al.*, "Microwave-based sensors with phthalocyanine films for acetone, ethanol and methanol detection," *Sensors and Actuators B: Chemical*, vol. 237, pp. 879-886, 2016.

[33] L. Grace, "The Effect of Moisture Contamination on the Relative Permittivity of Polymeric Composite Radar-Protecting Structures at X-band," *Composite Structures*, vol. 128, pp. 305-312, 2015.

[34] Z. Abbasi *et al.*, "Flexible Coupled Microwave Ring Resonators for Contactless Microbead Assisted Volatile Organic Compound Det., IEEE MTT-S Int. Microw. Symp. (IMS), Honolulu, USA, pp. 1228-1231, 2017.

[35] M. H. Zafiri *et al.*, "Detection of Volatile Organic Compounds Using Microwave Sensors," *IEEE Sensors Jour.*, vol. 15, no. 1, pp. 89-99, 2015.

[36] N. Wiwatcharagoses, K. Y. Parkm and P. Chahal, "Metamaterial-Inspired Sensor on Porous Substrate for Detection of Volatile Organic Compounds in Air, In Proceedings of the Electronic Components and Technology Conference", Las Vegas, USA, pp. 1557–1562, 2016.

[37] C. A. Balanis, *Antenna Theory: Analysis and Design*, second ed., New York, John Wiley & Sons., 1997.

[38] P. Fitl *et al.* "Laser deposition of sulfonated phthalocyanines for gas sensors" *Applied Surface Science,* vol. 302, pp. 37-41, 2014.

[39] D. Tomecek *et al.* "Phthalocyanine Photoregeneration for Low Power Consumption Chemiresistors" ACS Sensors, vol. 3, issue 12, pp. 2558 - 2565, 2018.

[40] Model DRH20 - Double ridge waveguide horn. RFspin s.r.o., June 2019. [Online]. Available at http://www.rfspin.cz/en/antennas/ /drh20.php.